IJMMM
International Journal of
Minerals, Metallurgy and Materials
矿物冶金与材料学报（英文版）

Preparation of crystalline rare earth carbonates with large particle size from the lixivium of weathered crust elution-deposited rare earth ores

Jing-qun Yin, Zhi-qiang Zou, and Jun Tian

Cite this article as:
Jing-qun Yin, Zhi-qiang Zou, and Jun Tian, Preparation of crystalline rare earth carbonates with large particle size from the lixivium of weathered crust elution-deposited rare earth ores, *Int. J. Miner. Metall. Mater.*, 27(2020), No. 11, pp. 1482-1488. https://doi.org/10.1007/s12613-020-2066-4

View the article online at SpringerLink or IJMMM Webpage.

Articles you may be interested in

Shuang Huang, Hua-lan Xu, Sheng-liang Zhong, and Lei Wang, Microwave hydrothermal synthesis and characterization of rare-earth stannate nanoparticles, *Int. J. Miner. Metall. Mater.*, 24(2017), No. 7, pp. 794-803. https://doi.org/10.1007/s12613-017-1463-9

Ping Long, Guan-shi Wang, Shuo Zhang, Shi-li Hu, and Ying Huang, A mathematical model for column leaching of ion adsorption-type rare earth ores, *Int. J. Miner. Metall. Mater.*, 27(2020), No. 4, pp. 463-471. https://doi.org/10.1007/s12613-019-1883-9

Shao-chun Chen, Hong-xiang Ye, and Xin-qiang Lin, Effect of rare earth and alloying elements on the thermal conductivity of austenitic medium manganese steel, *Int. J. Miner. Metall. Mater.*, 24(2017), No. 6, pp. 670-674. https://doi.org/10.1007/s12613-017-1449-7

Ze-yun Cai, Bo Song, Long-fei Li, Zhen Liu, and Xiao-kang Cui, Effect of CeO_2 on heat transfer and crystallization behavior of rare earth alloy steel mold fluxes, *Int. J. Miner. Metall. Mater.*, 26(2019), No. 5, pp. 565-572. https://doi.org/10.1007/s12613-019-1765-1

Gui-hua Liu, Zheng Li, Xiao-bin Li, Tian-gui Qi, Zhi-hong Peng, and Qiu-sheng Zhou, Precipitation of spherical boehmite from concentrated sodium aluminate solution by adding gibbsite as seed, *Int. J. Miner. Metall. Mater.*, 24(2017), No. 8, pp. 954-963. https://doi.org/10.1007/s12613-017-1483-5

Sayed Ghafar Hashemi B. Eghbali, Analysis of the formation conditions and characteristics of interphase and random vanadium precipitation in a low-carbon steel during isothermal heat treatment, *Int. J. Miner. Metall. Mater.*, 25(2018), No. 3, pp. 339-349. https://doi.org/10.1007/s12613-018-1577-8

IJMMM WeChat

QQ author group

International Journal of Minerals, Metallurgy and Materials
Volume 27, Number 11, November 2020, Page 1482
https://doi.org/10.1007/s12613-020-2066-4

Preparation of crystalline rare earth carbonates with large particle size from the lixivium of weathered crust elution-deposited rare earth ores

Jing-qun Yin[1)], *Zhi-qiang Zou*[2)], *and Jun Tian*[1)]

1) Institute of Applied Chemistry, Jiangxi Academy of Sciences, Nanchang 330029, China
2) School of Resource and Environmental Engineering, Jiangxi University of Science and Technology, Ganzhou 341000, China

(Received: 4 December 2019; revised: 13 April 2020; accepted: 15 April 2020)

Abstract: Crystalline rare-earth (RE) carbonates having large particle size were prepared from the lixivium of weathered crust elution-deposited rare-earth ores using the precipitation method with ammonium bicarbonate as the precipitant. Their chemical composition was studied using elemental and thermogravimetric analyses (TGA), and their structure and morphology were characterized using Fourier transform infrared (FTIR) spectroscopy, X-ray diffraction (XRD), and scanning electron microscopy (SEM). The results demonstrate that the crystalline rare-earth carbonate is a hydrated basic carbonate or oxycarbonate and not astable intermediate carbonate in the process of thermal decomposition. The particle size of crystalline rare-earth carbonates with large particle size is in the range of 50–200 μm. With an RE_2O_3 content of up to 95wt%, the quality of crystalline rare-earth carbonates is higher compared to the Chinese National Standard (GB/T 28882–2012). The quality of the product is superior to the Chinese National Standard.

Keywords: rare-earth ores; precipitation; crystalline rare-earth carbonate; large particle size

1. Introduction

The weathered crust elution-deposited rare-earth ores are reported in China [1] and constitute the primary resources of mid-heavy rare-earth (RE) elements in the world [2–3]. The rare-earth element in the ores is primarily found in the form of ions adsorbed on clay minerals [4], which can be leached using an electrolyte solution such as $(NH_4)_2SO_4$ and NH_4Cl [5–6]. The weathered crust elution-deposited ore is a type of clay mineral that co-exists with other elements and is characterized by complex components and relatively low-grade RE_2O_3. After leaching, using a solution of ammonium sulfate, the complex components are contained in the lixivium, a result of the electrolyte leaching [7]. Therefore, the composition of rare-earth lixivium is extremely complex and except for a low concentration of RE^{3+}, usually contains certain impurities such as $(NH_4)_2SO_4$ (~2000 mg/L), Al^{3+} (~1000 mg/L), Fe^{3+} (~100 mg/L), and Ca^{2+} (~1000 mg/L), along with a small amount of Fe^{2+}, Pb^{2+}, and Mn^{2+}, including the remaining lixiviants [8–9].

The extraction of rare-earth elements from this type of lixivium is achieved either by a chemical precipitation process or a non-precipitation process [10]. The process of extracting rare-earth elements from this type of lixivium, a common industry practice, is usually a chemical precipitation process with ammonium bicarbonate used as the precipitant, which includes washing, filtering, and drying and results in the forming of a rare-earth carbonate [11–13].

However, these precipitation technologies are complicated, tedious, and reagent-consuming [14], and the solid–liquid separation process is difficult. The impurities are co-precipitated with rare-earth elements and result in the low quality of the products, while the rare-earth yield is low [15]. Recently, the resources of weathered crust elution-deposited rare earth ores become poorer and the impurity in the ores becomes more complicated, therefore the content and the complexity of impurity in lixivium is constantly increasing [16]. The crystalline rate-earth carbonates are the well-crystallized precipitation of rare-earth carbonates using some kind precipitation process. The crystalline rare-earth carbonate with large particle size has the advantages of high product purity, good filterability, ease in washing, and high yield. However,

---

Corresponding author: Jun Tian E-mail: tianjun63@126.com

normal RE carbonate is a precipitate of amorphous structure. The precipitate is characterized by bad filterability, the product purity is low, and it is difficult to wash [17]. Therefore, the preparation of a crystalline rare-earth carbonate with large particle size from the lixivium of such a complexity is of considerable interest [18].

The preparation of crystalline rare-earth carbonates has been the object of previous studies [19]. The preparation of crystalline mixed rare-earth carbonates has been studied using $Mg(HCO_3)_2$ as the precipitant [18]. Moreover, the preparation of crystalline rare-earth carbonate from the lixivium of weathered crust elution-deposited rare earth ores has been studied [20]. Note that the preparation of crystalline rare-earth carbonates with large particle size from the lixivium of weathered crust elution-deposited rare earth ores using ammonium bicarbonate as the precipitant constitutes a new approach.

The precipitation processes of crystalline rare-earth carbonates with large particle size can increase the precipitating rate of rare-earth elements and the purity of the rare-earth product, which is practically beneficial for producing rare-earth elements and can constitute the ammonium bicarbonate method as a widely applied approach [20]. This is in accordance with the development trend of green chemistry.

2. Experimental

2.1. Characterization of the lixivium

The primary chemical components of the lixivium samples are listed in Table 1. REO is the rare-earth ores.

Table 1. Chemical components of the lixivium samples

mg·L^{-1}

K	Mg	Ca	Al	Fe	Mn
156	16.8	83.2	9.10	1.73	5.95
Pb	Zn	Si	pH	$(NH_4)_2SO_4$	REO
5.85	0.48	11.5	4.95	4.95	2150

The impurities affect both the rare-earth precipitating rate and the consumed precipitant and the purity of the RE carbonate product, particularly because of the failure of forming a crystalline RE precipitate. The formation of the crystalline RE carbonate is significantly affected by lixivium's components [21].

The partitioning of rare-earth elements in lixivium has been determined by Jiangxi Analytical and Testing Center, Nanchang, China, using inductively coupled plasma mass spectrometry (ICP−MS, SCIEX ELAN 9000 type) [22]. The result of the analysis is shown in Table 2.

Table 2. Partitioning of rare-earth elements in the lixivium [22]

wt%

La_2O_3	CeO_2	Pr_6O_{11}	Nd_2O_3	Sm_2O_3	Eu_2O_3	Gd_2O_3	Tb_4O_7
1.56	0.085	0.65	3.20	2.42	0.50	4.48	0.95
Dy_2O_3	Ho_2O_3	Er_2O_3	Tm_2O_3	Yb_2O_3	Lu_2O_3	Y_2O_3	
6.90	1.56	4.33	0.55	3.48	0.50	68.94	

As shown in Table 2, the partitioning of rare-earth elements in lixivium primarily contains middle rare earth (MRE) and heavy rare earth (HRE) elements.

2.2. Experimental procedure

The experimental procedure is as follows. Firstly, 50 mL of rare-earth lixivium was stirred continuously in the reactor and dropped on to an aliquot of ammonium carbonate solution at room temperature. The whiter rare-earth carbonates precipitations can form by adding an appropriate amount of crystallization nucleus and laid overnight. The rare-earth carbonate precipitation particle is gradually becoming larger. This behavior is typical of the crystalline process [23].

In this experiment, to optimize the process of rare-earth carbonation, the precipitation conditions include the following: the rare-earth contents in lixivium of 0.3 g/L, the concentration of ammonium bicarbonate of 2wt%, the stirring speed of 300 r/min, the precipitation reaction temperature of 60°C, and addition of crystal seed of 0.4 g/L. Finally, after precipitation, the products must be laid overnight.

Furthermore, the precipitation was separated by filtration, washed with ion exchange water, and dried at 105°C for more than 2 h. The large-sized particles and the crystalline shape of rare-earth carbonate can be obtained by strictly controlling the optimal precipitation process conditions such as the stirring intensity, the precipitation reaction temperature, the reactant ratio ($[NH_4HCO_3]/[REO]$ molar ratio), the concentration of rare-earth elements, the impurity content, and the amount of crystal seeds added.

2.3. Analytical methods

The content of rare-earth elements in lixivium was determined by EDTA (ethylenediamine tetraacetic acid) volumetric titration methods: α-benzoin oxime was used to precipitate heavy metal ions, acetylacetone was used to mask aluminum ion, ascorbicacid was used to reduce ferric iron to ferrous iron, and sulfosalicylic acid was used to mask ferrous iron. For using hexamethylenetetramine as a buffer and xylenol-orange as an indicator, titration with EDTA was used to analyze the concentration of rare-earth elements [22]. The content of rare-earth ore in the crystalline RE carbonate product was determined by the gravimetric method of oxalic acid precipitation, according to the national standard [24]. The impurity of the crystalline RE carbonate product was determined by the spectrophotometry method using o-phenanthroline, chromazurine, and silicomolybdic-blue [25]. The rare-earth partitioning of the ore samples was determined using inductively coupled plasma mass spectrometry (ICP–MS) [22]. Moreover, the thermogravimetric (TG) analysis of the crystalline rare-earth carbonate was performed on a TG209F3Tarsus® thermal gravimetric analyzer (NETZSCH TG 209F3, NETZSCH, Germany) at a heating rate of 10°C/min, temperature ranging from room temperature to 800°C, and a dynamic air flow of 60 mL/min. The crystalline rare-earth carbonate sample mass was 1.2218 mg, which was placed in corundum crucibles and heated. All the records were corrected using the baseline subtraction (a run without samples under the same conditions).

2.4. Characterization methods

The crystalline rare-earth carbonates were characterized by a Fourier transform infrared spectrometer (FTIR, Nicolet FTIR-7600, Nicolet Co., Ltd.). The test specimens were prepared using the KBr-disk method with thin (>20 mg/m^2), lightly loaded (<1%), KBr-supported (KBr, spectroscopy grade) discs. The FTIR spectra were obtained at a resolution of 4 cm^{-1} over the range between 4000 and 400 cm^{-1}.

An X-ray diffraction analysis (XRD) of the samples was performed using a powder X-ray diffractometer (Shimadzu XRD-7000, Shimazu, Japan) at a room temperature with scanning step of 0.1° in the 2θ range of 10°–80° (Cu K$_\alpha$ 1 monochromator camera radiation). The scanning electron microscope (SEM) images of the crystalline rare-earth carbonates were determined by Jiangxi academy of sciences analysis and test center with JSM-6460LV.

3. Results and discussion

3.1. Solution chemistry and precipitation reaction of ammonium bicarbonate and RE^{3+}

When ammonium bicarbonate was dissolved in water, hydrolysis and ionization occurred in the solution; the equilibrium of which can be described as follows [26]:

$$NH_4HCO_3 \Leftrightarrow NH_4^+ + HCO_3^- \tag{1}$$

$$NH_4^+ + H_2O \Leftrightarrow NH_3 \cdot H_2O + H^+ \tag{2}$$

$$K_{NH_4^+} = \frac{[NH_3]\cdot[H^+]}{[NH_4^+]} = 5.4\times10^{-10} \tag{3}$$

$$HCO_3^- + H_2O \Leftrightarrow H_2CO_3 + OH^- \tag{4}$$

$$K_A = \frac{[H_2CO_3]\cdot[OH^-]}{[HCO_3^-]} = 3.5\times10^{-7} \tag{5}$$

$$H_2CO_3 \Leftrightarrow HCO_3^- + H^+ \tag{6}$$

$$K_1 = \frac{[HCO_3^-]\cdot[H^+]}{[H_2CO_3]} = 4.2\times10^{-7} \tag{7}$$

$$HCO_3^- \Leftrightarrow CO_3^{2-} + H^+ \tag{8}$$

$$K_2 = \frac{[CO_3^{2-}]\cdot[H^+]}{[HCO_3^-]} = 5.6\times10^{-11} \tag{9}$$

Ammonium bicarbonate, which is formed by both a weak acid and base, can be ignored in the solution because it can easily hydrolyze in water. The total concentration of ammonium in water is as follows:

$$2HCO_3^- \Leftrightarrow CO_3^{2-} + H_2CO_3 \tag{10}$$

where Φ_0, Φ_1, and Φ_2 are the molar fractions of each component in the ammonium solution:

$$\Phi_0 = \frac{[CO_3^{2-}]}{[HCO_3^-]} = \frac{[CO_3^{2-}]}{[CO_3^{2-}]+[HCO_3^-]_S+[H_2CO_3]_S} = \frac{K_1K_2}{[H^+]^2+K_1[H^+]+K_1K_2} \tag{11}$$

$$\Phi_1 = \frac{K_1[H^+]}{[H^+]^2+K_1[H^+]+K_1K_2} \tag{12}$$

$$\Phi_2 = \frac{[H^+]^2}{[H^+]^2+K_1[H^+]+K_1K_2} \tag{13}$$

Fig. 1 shows the Φ–pH diagram of the water solution of carbonic acid system with K_1 and K_2.

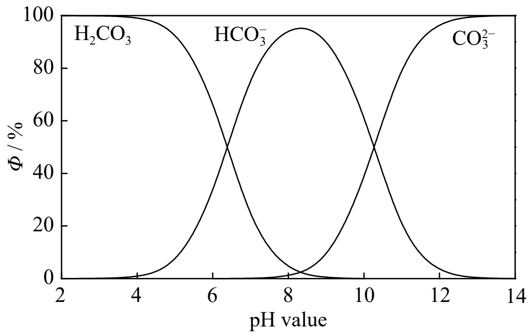

Fig. 1. Φ–pH diagram of carbonic acid system.

As shown in Fig.1, ammonium bicarbonate exists as CO_3^{2-} in water only at a high pH value. The precipitation reaction of rare-earth ions (RE^{3+}) with ammonium bicarbonate is expressed as follows [7]:

$$2RE^{3+} + 3HCO_3^- = RE_2(CO_3)_3\downarrow + 3H^+ \tag{14}$$

$$H^+ + HCO_3^- = CO_2\uparrow + H_2O \tag{15}$$

Combining the above two equations confirms the following:

$$2RE^{3+} + 6HCO_3^- = RE_2(CO_3)_3\downarrow + 3CO_2\uparrow + 3H_2O \tag{16}$$

Although the precipitate produced by the ammonium bicarbonate with RE ions is the normal carbonate, sometimes the basic carbonate may be formed because the carbonate tends to hydrolyze during precipitation. The formation tendency of the basic carbonate increases with increase in the atomic number [27].

Note that lixivium is characterized by fewer impurities and when concentration of rare-earth elements ranges between 0.1 and 0.5 g/L, crystalline rare-earth carbonates [$RE_2(CO_3)_3 \cdot 7H_2O$] with large particle size can be obtained under certain precipitation reaction conditions, namely, a pH value of 5–8, a temperature of 40–70°C, a raw material ratio of 1:0.8–1:16, stirring speed of 300–500 r/min, and an addition of crystal seed used as a guiding agent. These precipitation conditions favor the growth of large particle size crystals.

3.2. XRD analysis of the crystalline rare-earth carbonate

Fig. 2 shows the X-ray powder diffraction (XRD) pattern of the rare-earth carbonate precipitate [28]. As shown in Fig. 2, the diffraction peaks of the XRD pattern of the crystalline rare-earth carbonate are very high; its peaks are narrow and long, which indicates that the crystallization of the products is better, the crystalline form is perfect, and the structure of the crystal grain is larger [29]. The characteristic position and intensity of XRD peaks are consistent with that of $Y_2(CO_3)_3$ (JCPDS NO. 24-1419). The product was in a pure crystalline phase. It has confirmed the crystalline rare-earth carbonate as $Ln_2(CO_3)_3 \cdot nH_2O$. Therefore, the crystalline rare-earth carbonate has lesser crystalline surface energy, which means lower adsorption of impurities ions and which makes filtering and washing easier [30].

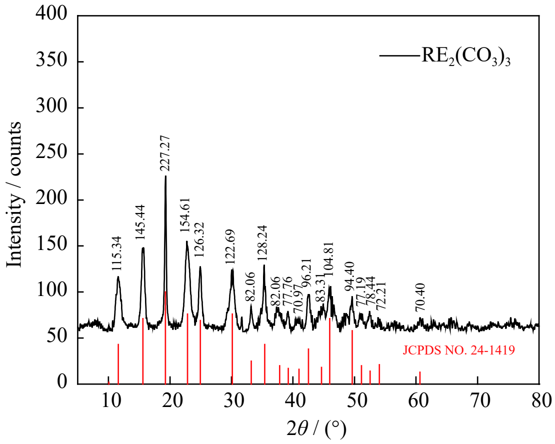

Fig. 2. XRD pattern of the crystalline rare-earth carbonate with a large particle size.

3.3. SEM analysis of the crystalline rare-earth carbonate with large particle size

Fig. 3 shows the SEM image of the crystalline rare-earth carbonate with large particle size. As shown in Fig. 3, the crystalline rare-earth carbonates particles are shown as the aggregation of multiple needle-shaped particles [31]. The particle size of the crystalline RE carbonates is estimated in the range of 50–200 μm, which indicates large size particles. This behavior is attributed to the effect of removing the impurities from the lixivium and to the fact that the concentration of rare-earth elements is relative to a dilute solution, under a certain optimization of the precipitation conditions, namely, pH, temperature, raw material ratio, stirring speed, and addition of crystal seed as a guiding agent. It is easy to filter when there are particles of large size and a crystalline shape [32].

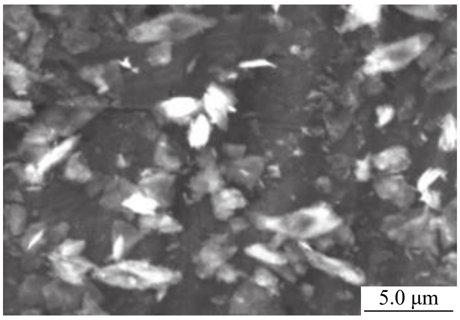

Fig. 3. SEM image of the crystalline rare-earth carbonates with large particle size.

3.4. FTIR analysis of the crystalline rare-earth carbonate

Fig. 4 shows the FTIR spectra of the crystalline rare-earth carbonate. Fig. 4 shows that the broad absorption band of ~3401 cm^{-1}, corresponding to O–H stretching and H–O–H bending vibrations, was present, which may be attributed to the water adsorbed in the surface [33]. The strong broad absorption band peaks at 1511 and 1418 cm^{-1} are the characteristic absorption peaks of CO_3^{2-} stretching vibration for $RE_2(CO_3)_3 \cdot 7H_2O$. The emergence of three peaks at 837.1, 761.2, and 687.4 cm^{-1} is attributed to the bending vibration of the $-CO_3^{2-}$ group. The characteristic absorbance bands at ~595.9 cm^{-1} indicate the RE–O stretching vibration. This infrared spectrum characteristic confirms that the target molecule is $RE_2(CO_3)_3 \cdot 7H_2O$.

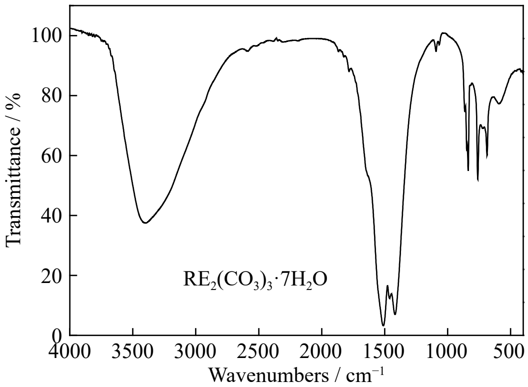

Fig. 4. FTIR spectra of the crystalline rare-earth carbonate with large particle size.

3.5. Thermal decomposition features of rare-earth carbonates with large particle size

Thermal decomposition of the crystalline rare-earth carbonates with large particle size was investigated using thermogravimetry [34]. Fig. 5 shows the thermogravimetric (TG) analysis from room temperature to 800°C.

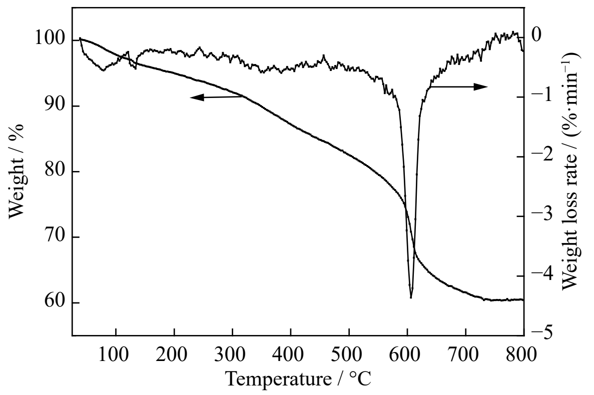

Fig. 5. Thermogravimetric plot of the crystalline rare earth carbonates with large particle size.

Fig. 5 also shows that the primary stages of thermal decomposition of the crystalline rare-earth carbonate in air are as follows [35]:

(1) At 50–150°C, dehydration of the crystalline rare earth carbonate:

$$RE_2(CO_3)_3 \cdot 7H_2O = RE_2(CO_3)_3 + 7H_2O \tag{17}$$

(2) At 607°C, decomposition of the anhydrous rare-earth carbonate:

$$RE_2(CO_3)_3 = RE_2O_3 + 3CO_2 \tag{18}$$

The lowest DTG (Derivative thermogravimetry) value obtained at 607°C shows the decomposition peak value. This point refers to the highest weight loss rate and signifies the decomposition of the anhydrous rare-earth carbonate.

3.6. Chemical composition and quality of the crystalline rare-earth carbonates

The elements of crystalline rare-earth carbonates have been subjected to chemical analysis and their chemical compositions are shown in Table 3.

Table 3. Chemical compositions of the crystalline rare-earth carbonates with large particle size wt%

Value type	RE_2O_3	CO_2	H_2O
Calculated	51.03	23.59	22.52
Measured	49.50	22.65	21.62

Note: The average molecular weight of rare-earth elements is 126.74, which is in accordance with the analysis of the rare-earth partition.

The data in Table 3 show that the chemical composition of the crystalline rare-earth carbonates is $RE_2(CO_3)_3 \cdot 7H_2O$ and that the precipitates products are target molecules [36]. When the crystalline rare-earth carbonates have been heated at 800°C for 2 h, the REO products are formed as REO. The product quality of the latter was analyzed according to the Chinese National Standard of rare-earth carbonate of ion-absorpted type rare-earth ore (GB/T 28882–2012) [37]; it is shown in Table 4.

Table 4. Quality of the crystalline rare earth carbonate with large particle size products wt%

Sample No.	REO	SiO_2/REO	Fe_2O_3/REO	Al_2O_3/REO	SO_4^{2-}	Ammonia-N	Loss on ignition
193212A	>92	<0.5	<0.2	<1.5	<0.5	<0.2	<75
REO	95.64	0.3	0.17	0.81	0.49	0.10	50.14

The data in Table 4 show that the quality of products of crystalline rare-earth carbonate is superior compared to the Chinese National Standard (GB/T 28882–2012). With content of ammonia-N being <0.2wt%, it is shown that the precipitate products are normal RE carbonates rather than ammonium and rare-earth carbonate compounds.

However, although the precipitation of crystalline rare-earth carbonates with large particle size has many advantages and the traditional chemical precipitation method has many disadvantages, industrial production still uses the latter because of its easiness in operation.

4. Conclusion

Crystalline rare-earth carbonates with a large particle size were prepared using the precipitation method from the lixivium of weathered crust elution-deposited rare-earth ores using ammonium bicarbonate as the precipitant. The chemical composition was studied by elemental analysis and thermogravimetry analysis. Note that both structure and morphology were characterized using FTIR, XRD, and SEM. The results show that the crystalline rare-earth carbonates have crystalline shape and large particle size, which is advantageous to the separating, filtering, and washing stages of the process. Furthermore, crystalline rare-earth carbonates contain less number of impurities, which is advantageous for reducing the precipitant consumption. The quality of the products of the crystalline rare-earth carbonates with large particle size was better than the Chinese National Standard (GB/T 28882–2012), with an RE_2O_3 content up to 95wt%.

Acknowledgements

This work was financially supported by the National Natural Science Foundation of China (Nos. 51964021 and 51774156), the Jiangxi Province Nature Science Foundation, China (No. 20181BAB206020), and China's National Key R & D Plan Project (No. 2019YFC0605000).

References

[1] G.A. Moldoveanu and V.G. Papangelakis, An overview of rare-earth recovery by ion-exchange leaching from ion-adsorption clays of various origins, *Mineral. Mag.*, 80(2016), No. 1, p. 63.

[2] Y. Kanazawa and M. Kamitani, Rare earth minerals and resources in the world, *J. Alloys Compd.*, 408-412(2006), p. 1339.

[3] K.M. Goodenough, F. Wall, and D. Merriman, The rare earth elements: Demand, global resources, and challenges for resourcing future generations, *Nat. Resour. Res.*, 27(2018), No. 2, p. 201.

[4] R.A. Chi, J. Tian, Z.J. Li, C. Peng, Y.X. Wu, S.R. Li, C.W. Wang, and Z.J. Zhou, Existing state and partitioning of rare earth on weathered ores, *J. Rare Earths*, 23(2005), No. 6, p. 756.

[5] L.Y. He, T.Z. Feng, S.Y. Fu, and D.X. Zhu, Study on process of extraction of rare earths from the ion-adsorption type rare earth ore ore by $(NH_4)_2SO_4$ leaching, *Chin. Rare Earths*, 4(1983), No. 3, p. 1.

[6] G.A. Moldoveanu and V.G. Papangelakis, Recovery of rare earth elements adsorbed on clay minerals: I. Desorption mechanism, *Hydrometallurgy*, 117-118(2012), p. 71.

[7] R.A. Chi and J. Tian, *Weathered Crust Elution-Deposited Rare Earth Ores*, Nova Science Publishers, Inc., New York, 2008.

[8] C. Bazin, K. El-Ouassiti, and V. Ouellet, Sequential leaching for the recovery of alumina from a Canadian clay, *Hydrometallurgy*, 88(2007), No. 1-4, p. 196.

[9] Y.X. Li, X.B. He, Z.Y. Gu, and P.G. Hu, Precipitation reaction of $RECl_3$ with NH_4HCO_3 and co-precipitation behavior of accompanying impurity Ions, *Chin. Rare Earths*, 20(1999), No. 2, p. 19.

[10] J. Tian, J.Q. Yin, K.H. Chen, G.H. Rao, M.T. Jiang, and R.A. Chi, Extraction of rare earths from the leach liquor of the weathered crust elution-deposited rare earth ore with non-precipitation, *Int. J. Miner. Process.*, 98(2011), No. 3-4, p. 125.

[11] R. Chi, Z. Zhou, Z. Xu, G. Zhu, and S. Xu, Solution-chemistry analysis of ammonium bicarbonate consumption in rare-earth-element precipitation, *Metall. Mater. Trans. B*, 34(2003), No. 5, p. 611.

[12] R. Chi and Z. Xu, A solution chemistry approach to the study of rare earth element precipitation by oxalic acid, *Metall. Mater. Trans. B*, 30(1999), No. 2, p. 189.

[13] Z.Y. Leng, S.Z. Liu, Y. Ma, Y.H. Xu, W.B. Wang, X.K. Hao, Y. Bai, M.Y. Fan, J.M. Huang, and Z. Wu, Crystalline rare earth carbonate precipitating from leaching solution of sulfuric acid calcinating concentrate of rare earth, *J. Rare Earths*, 21(2000), No. 2, p. 26.

[14] China Ministry of Environmental Protection, Chinese National Standard GB 26451–2011: *Emission Standards of Pollutants from Rare Earths Industry*, 2011.

[15] D.Q. Li, Chemical engineering problems in hydrometallurgical industry of rare earths, *Prog. Chem.*, 7(1995), No. 3, p. 209.

[16] X.P. Luo, L.P. Zou, P.L. Ma, C.G. Luo, J. Xu, and X.K. Tang, Removing aluminum from a low-concentration lixivium of weathered crust elution-deposited rare earth ore with neutralizing hydrolysis, *Rare Met.*, 36(2017), No. 8, p. 685.

[17] Z.H. Yu, M. Wang, L.S. Wang, L.S. Zhao, Z.Y. Feng, X. Sun, and X.W. Huang, Preparation of crystalline mixed rare earth carbonates by $Mg(HCO_3)_2$ precipitation method, *J. Rare Earths*, 38(2020), No. 3, p. 292.

[18] K. Michiba, T. Tahara, I. Nakai, R. Miyawaki, and S. Matsubara, Crystal structure of hexagonal $RE(CO_3)OH$, *Z. Kristallogr.*, 226(2011), No. 6, p. 518.

[19] Q.H. Yu and X.B. Li, Study on the formation of crystalline rare earth carbonates from rare earth ore leaching liquors, *J. Rare Earths*, 11(1993), No. 3, p. 223.

[20] J.Q. Yin and S.L. Lu, Preparation of crystalline carbonate rare earth from the controlled-flow rate elution leach liquid of the weathered crust elution-deposited rare earth ore, *Hydrometallurgy*, 14(1995), No. 4, p. 9.

[21] Y.H. Liu, J. Chen, and D.Q. Li, Application and perspective of ionic liquids on rare earths green separation, *Sep. Sci. Technol.*, 47(2012), No. 2, p. 223.

[22] J. Tian, J.Q. Yin, R.A. Chi, G.H. Rao, M.T. Jiang, and K.X. Ouyang, Kinetics on leaching rare earth from the weathered crust elution-deposited rare earth ores with ammonium sulfate solution, *Hydrometallurgy*, 101(2010), No. 3-4, p. 166.

[23] Z.Y. Xu, Y.J. Zhang, Z.Y. Fang, X.B. Yin, and W. Zhu, Controllable synthesis and optical properties of $NdOHCO_3$ dodecahedral microcrystals, *Mater. Res. Bull.*, 45(2010), No. 1, p. 74.

[24] General Administration of Quality Supervision, Inspection and Quarantine of the People's Republic of China, Chinese National Standard GB/T 18882.1–2002: *Chemical Analysis Methods for Mixed Rare Earth Oxide of Ion-absorpted Type RE Ore-Determination of Total Rare Earth Contents-Oxalate Gravimetric Method*, 2002.

[25] J. Tian, J.Q. Yin, X.K. Tang, J. Chen, X.P. Luo, and G.H. Rao, Enhanced leaching process of a low-grade weathered crust elution-deposited rare earth ore with carboxymethyl sesbania gum, *Hydrometallurgy*, 139(2013), p. 124.

[26] A.B. Ali, V. Maisonneuve, S. Houlbert, G. Silly, J.Y. Buzaré, and M. Leblanc, Cation and anion disorder in new cubic rare earth carbonates $Na_2LiLn(CO_3)_3$ (Ln = Eu-Er, Yb, Lu, Y); synthesis, crystal structures, IR, Raman and NMR characterizations, *Solid State Sci.*, 6(2004), No. 11, p. 1237.

[27] M.S. Refat, A novel method for the synthesis of rare earth carbonates, *Synth. React. Inorg. Met.-Org. Chem.*, 34(2004), No. 9, p. 1605.

[28] H.S. Sheu, W.J. Shih, W.T. Chuang, I.F. Li, and C.S. Yeh, Crystal structure and phase transitions of $Gd(CO_3)OH$ studied by synchrotron powder diffraction, *J. Chin. Chem. Soc.*, 57(2010), No. 4B, p. 938.

[29] B. Want, Single crystal growth and characterization of lanthanum–neodymium oxalate octahydrate, *J. Cryst. Growth*, 335(2011), No. 1, p. 90.

[30] S. Liu and R.J. Ma, Preparation of crystalline precipitation of mixed rare earth carbonates, *Chin. J. Nonferrous Met.*, 8(1998), No. 2, p. 331.

[31] F.B. Gu, Z.H. Wang, D.M. Han, G.S. Guo, and H.Y. Guo, Crystallization of rare earth carbonate nanostructures in the reverse micelle system, *Cryst. Growth Des.*, 7(2007), No. 8, p. 1452.

[32] Y.J. Zhang, H.M. He, X.Z. Yang, A. Zheng, and Y. Fan, Morphology-controlled synthesis, characterization, growth mechanism of $SmOHCO_3$ with high uniform size and photoluminescence property of $SmOHCO_3$:Eu^{3+}, *Powder Technol.*, 224 (2012), p. 175.

[33] R.L. Frost, Y.F. Xi, R. Scholz, F.M. Belotti, and M.C. Filho, Infrared and Raman spectroscopic characterization of the carbonate mineral weloganite-$Sr_3Na_2Zr(CO_3)_6\cdot 3H_2O$ and in comparis-

on with selected carbonates, *J. Mol. Struct.*, 1039(2013), p. 101.

[34] N.N. Bushuev and D.S. Zinin, Thermal decomposition features of calcium and rare-earth oxalates, *Russ. J. Inorg. Chem.*, 61(2016), No. 2, p. 161.

[35] G. Zhan, J.X. Yu, Z.G. Xu, F. Zhou, and R.A. Chi, Kinetics of thermal decomposition of lanthanum oxalate hydrate, *Trans. Nonferrous Met. Soc. China*, 22(2012), No. 4, p. 925.

[36] S.H. Yin, G. Lin, S.W. Li, J.H. Peng, and L.B. Zhang, Application of response surface methodology for optimization of parameters for microwave heating of rare earth carbonates, *High Temp. Mater. Processes*, 35(2016), No. 8, p. 813.

[37] General Administration of Quality Supervision, Inspection and Quarantine of the People's Republic of China, Standardization Administration of the People's Republic of China, Chinese National Standard GB/T 28882–2012: *Rare Earth Carbonate of Ion-absorpted Type Rare Earth Ore*, 2012.